R4 Dynamic Range Improvement by Narrow-Channel Effect Suppression and Smear Reduction Technologies in Small Pixel IT-CCD Image Sensors

A. Tanabe, Y. Kudoh, Y. Kawakami, K. Masubuchi, S. Kawai, T. Yamada, M. Morimoto*, K. Arai, K. Hatano**, M. Furumiya**, Y. Nakashiba**, N. Mutoh, K. Orihara, and N. Teranishi

Silicon Systems Research Labs., *System Micro Division, **ULSI Device Development Labs.
NEC Corporation
1120 Shimokuzawa, Sagamihara, Kanagawa 229-1198, Japan

Abstract

Technologies for narrow-channel effect suppression in photodiodes (PDs) and vertical CCDs (V-CCDs) and for smear reduction in PDs have been developed in order to improve dynamic range in small pixel interline-transfer CCD (IT-CCD) image sensors. The new technologies have been applied to a progressive-scan IT-CCD image sensor with 5 μm square pixels and have 1) increased the charge handling capability of its V-CCDs to 4500 electrons/V; 2) improved its smear value to -95 dB; and 3) increased the saturation charge of its PDs to 2.3×10^4 electrons.

Introduction

The strong demand for smaller image area as well as for improvement in resolution have created the need for smaller pixels, and, in fact, pixels as small as 5 μm square have already been reported for a recently developed 1/2 inch 1.3M pixel progressive-scan interline-transfer CCD (IT-CCD) image sensor (1). Pixel size reduction, however, results in a decrease in saturation signal and consequently a decrease in dynamic range, because it is inevitably accompanied by a reduction in photodiode (PD) and vertical CCD (V-CCD) areas.

While dynamic range can be increased by increasing the PD saturation charge, it is also critical to increase the V-CCD charge handling capability and to reduce smear at the same time because V-CCD charge handling capability must always be greater than the sum of the PD saturation charge and additional charges due to smear and vertical-overflow-drain (VOD) knee characteristics under high intensity light. Fig. 1 shows transferred charge in a V-CCD as a function of incident light intensity. Up to the PD saturation charge, the signal charge photogenerated at a PD is proportional to light intensity. Beyond the PD saturation charge, excess charge from a PD with a VOD structure is a logarithmic function of light intensity and is referred to as VOD knee. Other extra charge, accumulated at the V-CCD, is smear charge. The V-CCD charge handling capability, then, must be greater than the sum of the PD saturation charge, the VOD knee, and the smear charge. Furthermore, some margin is also needed because of fluctuation in the above mentioned charge characteristics due to variations in fabrication accuracy. That is to say, increasing V-CCD charge handling capability and reducing smear make it possible to increase PD saturation charge, and thus to improve dynamic range as well.

In order to increase dynamic range, the authors have developed two new technologies for IT-CCD image sensors. One is a narrow-channel effect suppression technology to increase both the PD saturation charge and the V-CCD charge handling capability. The other is a technology for smear reduction. These new technologies have been applied to a progressive-scan IT-CCD image sensor with 5 μm square pixels.

New Pixel Structure

Fig. 2 illustrates the new pixel structure. The unit pixel consists of the PD, the V-CCD, the transfer-gate (TG) region, and the P^+ channel stopper (CS). The one difference with the conventional structure is the two perimeter-N^+ regions introduced within both the PD N-layer and the V-CCD N-layer. The perimeter-N^+ regions narrow the width of the depletion region that extends from the edge of the P^+ channel stopper into the N-layers of both the PD and the V-CCD. A consequent widening of the charge accumulation region, described later, results in an increase in PD saturation charge and V-CCD charge handling capability. H. Shiraki et al. have proposed similar N^+ region design concept, but their structure itself is fundamentally different (2).

Another structural characteristic of our device is a shallower PD surface P^+ layer, created by BF_2 ion implantation. The shallow P^+ layer decreases the surface electron diffusion flow, one which is not included among the three origins generally

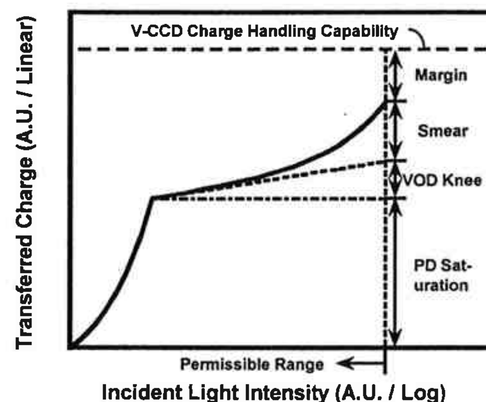

Fig. 1 Transferred charge in a V-CCD in terms of incident light intensity. Beyond saturation, charge consists of PD saturation charge and additional charge due to VOD knee effect and smear. V-CCD charge handling capability must be greater than the sum of the PD saturation charge and the additional charge.

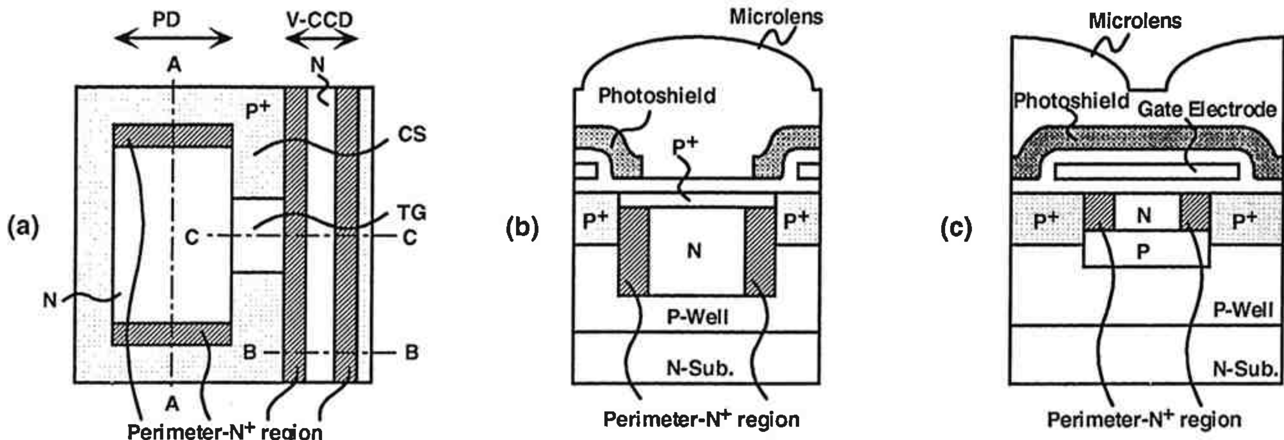

Fig. 2 The new pixel structure. (a) Top view of the new unit pixel. (b) Cross-sectional view of the PD taken along line A-A in (a). (c) Cross-sectional view of the V-CCD taken along line B-B in (a). The shallow P^+ layer in PD was made by BF_2 ion implantation; and the perimeter-N^+ regions are formed within both the PD N-layer and the V-CCD N-layer.

noted as being responsible for smear (3). As will be seen, decreasing this flow can decrease smear.

Improvement of V-CCD Charge Handling Capability

The effect of the two perimeter-N^+ regions in the V-CCD N-layer may be seen in Figs. 3, 4, and 5. As indicated by the simulated potential profile across the width of the V-CCD when its N-layer is depleted at the gate voltage (VG) of 0 V (see Fig. 3), potential in the new structure rises more sharply at the both sides than that in the conventional structure, which indicates a suppression of the narrow-channel effect. This has been confirmed by the measurements illustrated in Fig. 4, which show a channel potential for both the new and conventional structures as a function of V-CCD width. The channel potential drop by the narrow-channel effect seen in the conventional structure below 3 μm is very slight in the new structure. Fig. 5 shows a simulated potential profile across the width of the V-CCD taken along the same line as that of Fig. 3, when maximum charge has accumulated in the V-CCD N-layer. The charge accumulation region, where the potential is flat, in the new structure is wider than that of the conventional structure by approximately 20%. The resulting V-CCD charge handling capability per unit amplitude of the driving pulse-voltage is 4500 electrons/V, higher than that of the conventional structure by approximately 20%.

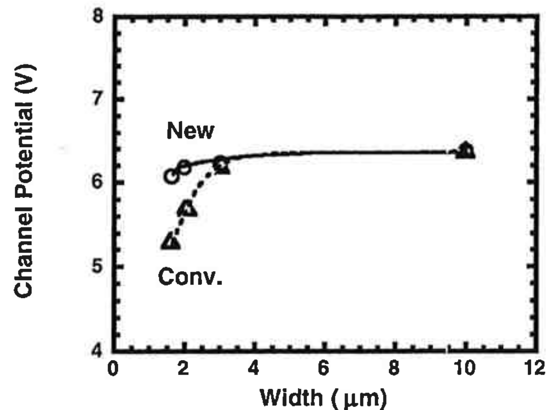

Fig. 4 Measured channel potential as a function of V-CCD width at VG=0 V, where width of the perimeter-N^+ region is kept constant.

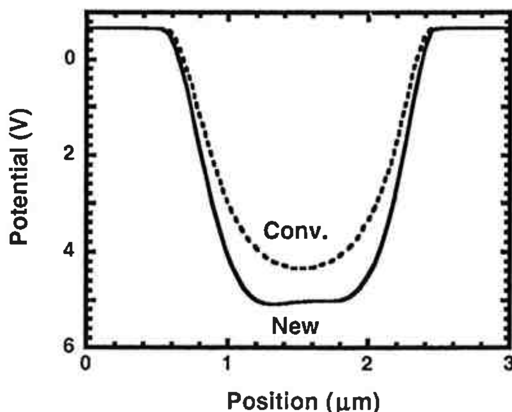

Fig. 3 Simulated potential profile taken along line B-B in Fig. 2 (a) when the V-CCD N-layer is completely depleted at VG=0 V. The narrow-channel effect is suppressed in the new structure.

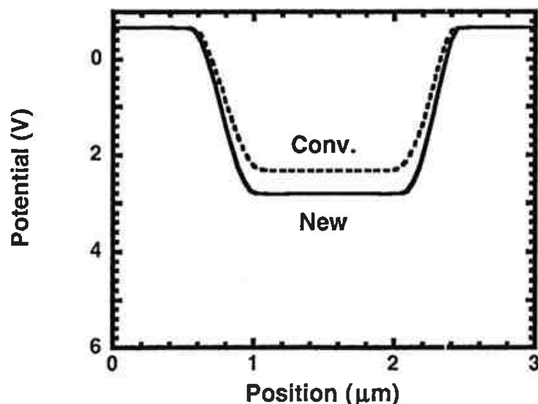

Fig. 5 Simulated potential profile taken along line B-B in Fig. 2 (a) when maximum charge has accumulated in the V-CCD N-layer at VG=0 V. The charge accumulation region, where potential is flat, is wider in the new structure.

Smear Reduction

The three generally noted origins of smear noise are: diffusion of electrons photogenerated in the P-well, light penetration through the photoshield, and light leakage (caused by, for example, a diffraction effect at the photoshield edge, a waveguide effect by which light passes through the dielectric layer under the photoshield, etc.) (3). In our device, however, the photoshield is thick enough to make penetration of it a negligible element, and the dielectric layer is made as thinner as possible to reduce the waveguide effect (4). With regard to eliminating the diffraction effect, the only method that we are aware of is that of extending photoshield coverage with respect to the V-CCD, but since this would reduce PD sensitivity, we can not sufficiently suppress this effect. Instead, we made diffusion of electrons, including that photogenerated in the P-well, the focus of our efforts to reduce smear.

We used a two-dimensional simulator to determine the paths followed by electrons photogenerated at the PD. This simulator can calculate diffusion of electrons photogenerated by the incident light but not include the diffraction effect and the waveguide effect. Fig. 6 shows a simulated electron flow profile under the perpendicularly incident light with 550 nm wavelength for a cross-sectional view taken along line C-C in Fig. 2, for both the new (a) and conventional structures (b). In each structure, electrons flow toward the V-CCD N-layer at the surface of the both photoshield edges (TG side and CS side), while electron diffusion flow from the P-well (upward arrows) to the V-CCD N-layer is slight. As may be seen on the left-hand sides of both Figs. 6 (a) and (b), however, surface electron flow near the TG region changes course to move into the PD N-layer at that area where it is not entirely covered by the surface P^+ layer, and the flow never reaches the V-CCD N-layer. By way of contrast, as may be seen on the right-hand sides of these figures, the surface electron flow in the PD P^+ layer goes to the V-CCD N-layer through the CS region. That is to say, smear noise from the CS side is dominant in the surface electron diffusion factor. Thinking that this electron flow might be decreased by reducing the thickness of the PD surface P^+ layer, we used BF_2 ion implantation to form the PD surface P^+ layer, with the result that this layer was only half the thickness of the conventional. Surface electron flow in this new structure decreased by approximately 97%.

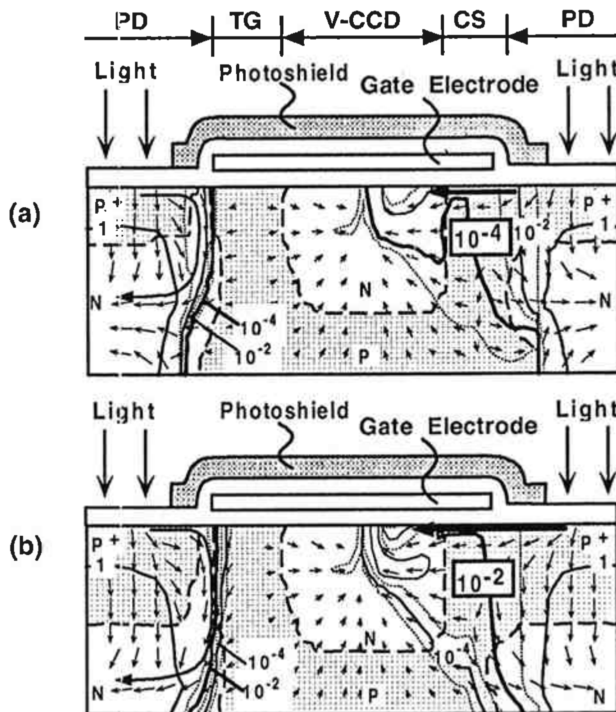

Fig. 6 Simulated electron flow profile for a cross-sectional view taken along line C-C in Fig. 2 (a) for the new structure (a) and for the conventional structure (b). The cross-sectional view shows the V-CCD at the center and its neighbor PDs at both sides. Values indicated are in arbitrary units. Small arrows indicate the direction of electron flow. Electrons photogenerated at the PD surface P^+ layer pass through the P^+ channel stopper to the V-CCD N-layer at the CS side by way of a newly found surface electron diffusion path.

Fig. 7 shows measured smear noise for both the new and conventional structures. The light source was 4300 K tungsten lamp and the optics of F8 with the IR cut filter. Smear noise from the TG side and that from the CS side are indicated separately. The smear noise from the CS side is larger than that of the TG side by about one order of magnitude in the conventional structure. Therefore, decreasing the smear noise from the CS side is necessary to decrease total smear noise. In the new structure, smear noise from the CS side is improved by approximately 9 dB over that of the conventional structure, mainly because the surface electron flow decreased to be a negligible level. On the other hand, smear noise from the TG side is almost the same in both the new and conventional structures, because the surface electron flow is negligible and smear noise caused by light leakage is the same. Total smear noise for the new structure is -95 dB, an improvement of approximately 7 dB over that of the conventional structure. This confirms that the surface electron diffusion path from the CS side is a significant factor in smear noise. Smear noise in the new structure must be caused by light leakage. To decrease smear noise further, light leakage must be reduced.

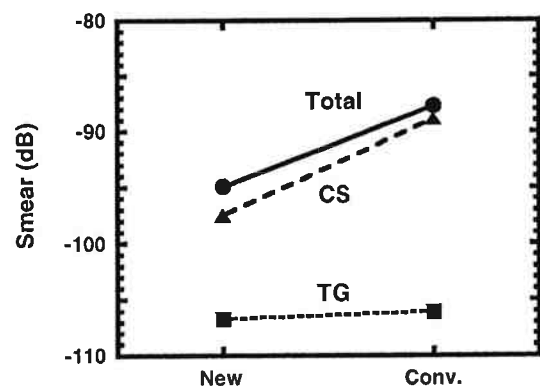

Fig. 7 Comparison of smear noise between the new and the conventional structures. The smear noise from the CS side is improved by approximately 9 dB, while that from the TG side is almost the same. Total smear noise of -95 dB is obtained in the new structure, an improvement of approximately 7 dB over that of the conventional structure.

Improvement of PD Saturation Charge

The effect of the two perimeter-N^+ regions, similar to those in the V-CCDs, in the PD N-layer may be seen in Figs. 8 and 9. As indicated by the potential profile, calculated by a three-dimensional simulator, across the width of the PD taken along line A-A in Fig. 2 (a) when its N-layer is completely depleted (see Fig. 8), the perimeter-N^+ regions have the same narrow-channel effect suppression as in the V-CCD. The measured PD saturation charge, electronic shutter pulse-voltage, and read-out voltage in the new structure are compared with those in the conventional structure in Fig. 9. The PD saturation charge of $2.3x10^4$ electrons is achieved in the new structure, which is approximately 40% higher than that in the conventional structure. This results in improvement in dynamic range by approximately 3 dB, since total noise as well as the dark current in the new structure was measured to be the same as those in the conventional structure. Moreover, the three-dimensional simulations show that the increase in potential over that of the conventional structure at the plateau in the completely depleted N-layer is so slight. This explains that the resulting increase in the measured read-out voltage and electronic shutter pulse-voltage are negligible. There was no difference in the measured VOD knee characteristics between the new and conventional structures. The VOD knee characteristics is related to the strength of capacitive coupling between the PD N-layer and the P-well (5). Increase in the capacitance between the PD N-layer and the P-well over that of the conventional structure may be little because the perimeter-N^+ regions are located at the edge of the PD N-layer and do not affect this capacitance. Therefore, there is no difference in the VOD knee characteristics between both structures.

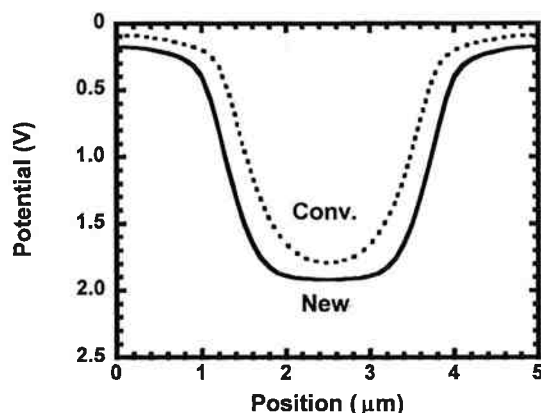

Fig. 8 Simulated potential profile taken along line A-A in Fig. 2 (a) when the PD N-layer is completely depleted. Suppressing the narrow-channel effect is the same as in V-CCDs.

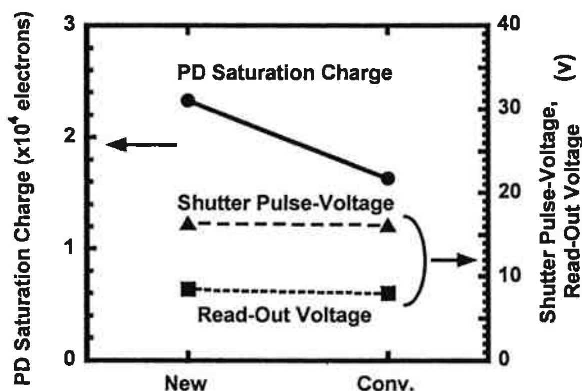

Fig. 9 Comparison of PD saturation charge, electronic shutter pulse-voltage, and read-out voltage between the new and conventional structures. In the new structure, the PD saturation charge increases by 40% over that of the conventional, while electronic shutter pulse-voltage and read-out voltage increase only negligibly.

Conclusion

The technologies for narrow-channel effect suppression in PDs and V-CCDs and for smear reduction in PDs have been developed in order to improve dynamic range in small pixel IT-CCD image sensors. In order to increase the PD saturation charge and the V-CCD charge handling capability, the perimeter-N^+ regions are introduced within both the PD N-layer and the V-CCD N-layer. This has the effect of suppressing the narrow-channel effect, consequently widening the charge accumulation region. In order to reduce smear, the shallower PD P^+ layer is created by BF_2 ion implantation. This has the effect of decreasing the surface electron diffusion flow at the CS side, which we discovered.

These new technologies have been applied to a progressive-scan IT-CCD image sensor with 5 μm square pixels and have 1) increased the charge handling capability of its V-CCDs to 4500 electrons/V; 2) improved its smear value to -95 dB; and 3) increased the saturation charge of its PDs to $2.3x10^4$ electrons. The dynamic range was increased by 3 dB, since total noise was the same as that in the conventional structure. These technologies do not cause any increase in driving voltages.

These newly developed technologies are quite effective for improving dynamic range in small pixel IT-CCD image sensors without increasing driving voltage and are especially promising for application to high-performance digital still cameras.

References

(1) T. Yamada et al., "A 1/2 inch 1.3M-pixel progressive-scan IT-CCD for still and motion picture applications," in *ISSCC Dig. Tech. Papers*, pp. 178-179, 1998.

(2) H. Shiraki and N. Ushijima, "A consideration on signal charge increase in the photodiodes with VOD structure," in *Proc. ITE Annual Convention*, pp.21-22, 1997 (in Japanese).

(3) H. Ono, T Ozaki, H Tanaka, and Y. Kawamoto, "Analysis of smear noise in interline-CCD image sensor with gate-free isolation structure," in *Ext. Abst. Int. Conf. on Solid State Devices and Materials*, pp. 68-70, 1991.

(4) N. Teranishi and Y. Ishihara, "Smear reduction in the interline CCD image sensor," *IEEE Trans. Electron Devices*, vol. ED-34, No. 5, pp. 1052-1056, 1987.

(5) S. Kawai, M. Morimoto, N. Mutoh, and N. Teranishi, "Photo response analysis in CCD image sensors with a VOD structure," *IEEE Trans. Electron Devices*, vol. 42, No. 4, pp. 652-655, 1995.